Signal Integrity verification of complex high-speed interconnects via Waveform Relaxation

Signal Integrity verification of complex high-speed interconnects via Waveform Relaxation

S. Grivet-Talocia, V. Loggia

Dip. Elettronica, Politecnico di Torino
C. Duca degli Abruzzi 24, 10129 Torino, Italy
Email: stefano.grivet@polito.it

***Abstract*—We present a Waveform Relaxation approach for fast transient simulation of electrically long high-speed channels. The proposed technique is based on a two-level transverse and longitudinal partition of the coupled interconnect. All couplings and feedback from terminations are represented as correction sources, which become explicit in a Waveform Relaxation framework. We show that the proposed schemes are consistent and allow for very efficient implementations. Simulation results show speedup factors of up to two orders of magnitude with respect to circuit-based (SPICE) solvers.**

I. Introduction

This paper presents a fast simulation technique for complex and electrically long coupled interconnects, terminated by possibly nonlinear drivers and receivers. Common examples for such structures are point-to-point links connecting different chips and routed through geometrically complex paths running through packages, printed circuit boards, connectors, etc. Signal Integrity verification of such systems via fast simulation is of paramount importance [1]-[4].

Electrical characterization of multi-chip links is usually available in form of tabulated frequency samples of their scattering matrix. These are available either from direct measurement or from simulations. In the latter case, the overall channel characterization is typically obtained by cascading individual scattering matrices for the single blocks forming the channel, such as connectors, via fields, or transmission line segments, which are computed using 2D or 3D field solvers [2]. Conversely, driver and receiver circuits are intrinsically nonlinear and require adequate representation, either as transistor-level circuits or as nonlinear behavioral macromodels. The above characteristics make the transient simulation of multi-chip links a quite challenging problem.

Various approaches are available for setting up a transient channel simulation [1], [2], [3], [4]. If the terminations are approximated by linear circuits, the entire solution can be performed in the frequency domain, and the transient termination voltages and currents can be derived as a postprocessing step via inverse Fourier Transform. The reliability of this approach is limited by the inexact representation of terminations. Alternatively, the transient scattering impulse responses of the channel can be computed via inverse Fourier transform, and the transient solution of the terminated channel can be obtained via convolution. This approach is numerically robust but can be slow. Alternative approaches are based on macromodeling techniques. The channel is first represented as an equivalent circuit, which is extracted by curve fitting with passivity constraints from the tabulated scattering data [6]-[14]. Once available, this circuit can be combined with terminations and directly solved with SPICE [13]. Unfortunately, also this approach may be too slow for the long transient simulations that are required for a detailed Signal Integrity verification.

In this work, we use a different approach. We also derive a macromodel for the channel, which is expressed in closed form as a combination of rational functions and delay operators in the Laplace domain [6]-[14]. Analytic Laplace transform inversion leads to a functional expression of the channel impulse responses, which allow to cast convolutions in a recursive form [5], or equivalently as IIR (Infinite Impulse Response) filters. These characteristics are exploited in a two-level Waveform Relaxation framework [16]-[30], where the overall simulation problem is split and approximated as a set of individual decoupled and simpler simulations, which require reduced computational cost. Convergence to the exact solution is recovered by applying relaxation sources, consisting of inter-channel couplings and reaction from terminations. Numerical results show that our preliminary implementation of the two-level WR scheme outperforms SPICE by more than two orders of magnitude in runtime, with the same level of accuracy.

II. Delayed-Rational Macromodels

We consider a fully-coupled P-port (P even) channel terminated by single-ended drivers and receivers. Figure 1a depicts this structure for the case $P = 4$. We make the assumption that the only coupling between different nets occurs within the channel, with no explicit coupling between individual drivers and receivers. This case is quite common in practical applications.

The channel is known from its sampled scattering matrix $\widehat{\mathbf{H}}_l \in \mathbb{C}^{P\times P}$ at the discrete frequencies $\omega_l,\ l = 1,\ldots,L$. The first step of our proposed technique is the derivation of a macromodel, which can be cast in a form suitable for transient analysis. We define as Delay-Rational Macromodel (DRM) [6]-[12] the Laplace-domain scattering matrix with

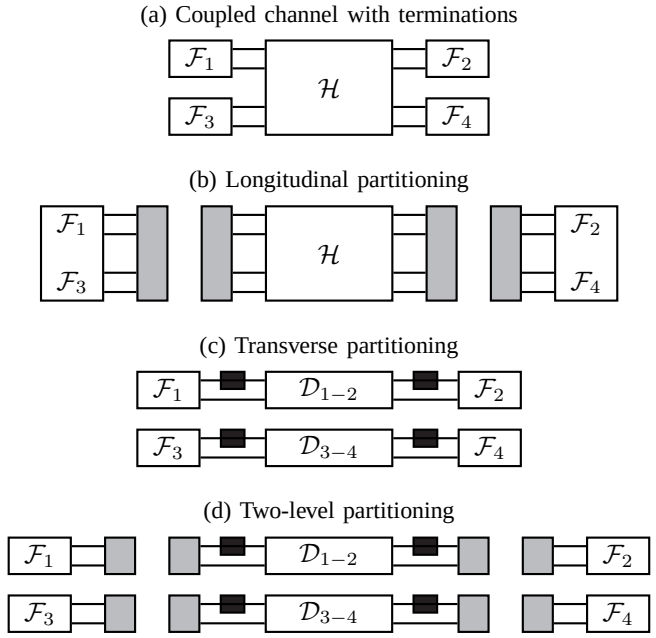

Fig. 1. System topology (a) and various partitioning schemes: longitudinal (b), transverse (c), and two-level (d). Light and dark gray boxes denote longitudinal and transverse decoupling and relaxation sources, respectively.

elements

$$H^{i,j}(s) = \sum_{m=0}^{M^{i,j}} \sum_{n=1}^{N_m^{i,j}} \frac{R_{mn}^{i,j}}{s - p_{mn}^{i,j}} e^{-s\tau_m^{i,j}} + D^{i,j} \tag{1}$$

where s is the Laplace variable, i, j denote output and input port, respectively, corresponding to the selected scattering response, $\tau_m^{i,j}$ are delays corresponding to the various arrival times of the signal reflections induced by an input unit pulse. The rational coefficients

$$Q_m^{i,j}(s) = \frac{R_{mn}^{i,j}}{s - p_{mn}^{i,j}} \tag{2}$$

are used to approximate attenuation and dispersion effects.

The identification of (1) from the samples $\widehat{\mathbf{H}}_l$, i.e., solving

$$\min \|\mathbf{H}(j\omega_l) - \widehat{\mathbf{H}}_l\| \,, \tag{3}$$

where the minimum is taken over the unknown delays $\tau_m^{i,j}$ and matrix rational functions $Q_m^{i,j}(s)$ is performed using the so-called Delayed Vector Fitting (DVF) [7], which is well documented and is not further commented here. We remark that also the passivity of (1) is easily checked and enforced, see [10], [12].

Analytic inversion of (1) can be carried out, leading to the impulse response

$$h^{i,j}(t) = \sum_{m=0}^{M^{i,j}} \sum_{n=1}^{N_m^{i,j}} R_{mn}^{i,j} \mathrm{e}^{p_{mn}^{i,j}\left(t-\tau_m^{i,j}\right)} u(t - \tau_m^{i,j}) + D^{i,j}\delta(t) \,, \tag{4}$$

which in turn can be used to compute the channel response $\boldsymbol{y}(t)$ due to any input signal $\boldsymbol{x}(t)$ through convolution $\boldsymbol{y}(t) = \mathbf{h}(t) * \boldsymbol{x}(t)$. Due to the exponential kernel, this convolution can be discretized on a uniform time grid $t_k = k\delta$ and approximated as a superposition of scalar three-tap Infinite Impulse Response filters. Dropping for simplicity superscripts ^{i,j} and restricting to the case of a single pole term (m, n fixed), we have

$$y(t_k) \simeq \alpha_0 y_{k-1} + \beta_0 x(t_{k-\bar{k}}) + \beta_1 x(t_{k-1-\bar{k}}) + \beta_2 x(t_{k-2-\bar{k}}) \,, \tag{5}$$

where coefficients α_0, $\beta_{0,1,2}$ depend on the pole p, residue R, and discretization time step δ, and where

$$\tau = \bar{k}\delta + \tau_\epsilon, \quad \text{where} \quad \bar{k} = \left\lfloor \frac{\tau}{\delta} \right\rfloor \tag{6}$$

denotes the integral part of the delay τ with a remainder $\tau_\epsilon < \delta$. A detailed derivation of (5) is available in [32].

The above formulation of the time-domain channel model can be cast in a compact operator notation. If we denote with $\boldsymbol{a}$ and $\boldsymbol{b}$ the vector-valued arrays collecting all time samples t_k, $k = 0, \ldots, K$ of the scattering signals that impinge into and are reflected from all channel ports, respectively, we have

$$\boldsymbol{b} = \mathcal{H}\,\boldsymbol{a} \,, \tag{7}$$

where each element of the matrix-valued operator $\mathcal{H}$ corresponds to a superposition of time-domain recursive convolutions (5). Application of this operator requires a computational cost that scales only linearly with the number of samples K.

We turn now to the formulation of the termination equations. The scattering wave $\boldsymbol{b}$ that is reflected by the channel is clearly the impinging wave into the terminations, viewed as a single multiport element. Therefore, we cast also the termination equations using a scattering representation as

$$\boldsymbol{a} = \mathcal{F}\,(\boldsymbol{b}) \,, \tag{8}$$

where operator $\mathcal{F}$ is diagonal (it couples only impinging and reflected waves at a single port) but can be nonlinear, dynamic and possibly include time-varying source terms as in the case of drivers. The compact notation (8) assumes that any differential terms in the termination equations have been suitably discretized over the assumed grid t_k.

III. System Partitioning and Waveform Relaxation

The direct solution of coupled equations (7) and (8) would require the direct solution of nonlinear equation

$$\boldsymbol{b} = \mathcal{H}\,\mathcal{F}\,(\boldsymbol{b}) \tag{9}$$

to be performed at each time step. This is what SPICE does, using Newton-Raphson iterations repeatedly. Here, we want to avoid any direct nonlinear solution and/or time-stepping iteration. This can be accomplished by system partitioning and Waveform Relaxation. The following three sections describe the proposed longitudinal, transverse, and combined system partitioniong schemes, which lead to corresponding Waveform Relaxation iterations. We remark that only the final two-level relaxation of Sec. III-C is interesting from the computational standpoint. The first two schemes are presented separately in order to illustrate the advantages of each partitioning strategy.

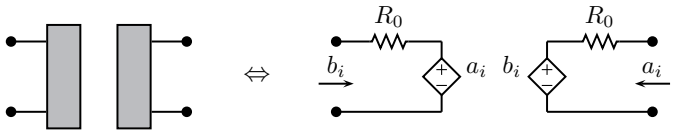

Fig. 2. Definition of the decoupling source for a single interface port.

A. Longitudinal Partitioning

Longitudinal partitioning involves a cut at all channel ports in order to separate the channel from its terminations. The hanging terminals are then connected to suitable decoupling networks, which ensure that the partitioned system is equivalent to the original. This condition is easily achieved by the circuits depicted in Fig. 2, where we used the definition $\{a, b\} = v \pm R_0 i$ of the (voltage) scattering waves in terms of port voltage and current. Panel (b) of Fig. 1 provides a graphical illustration of this process.

Waveform Relaxation is now introduced by using the decoupling blocks as relaxation sources. We define an iteration index ν and we relax the instantaneous coupling of the two equations (7) and (8) by delaying one of the terms by one iteration. The result is

$$\begin{cases} \boldsymbol{b}_\nu = \mathcal{H}\, \boldsymbol{a}_{\nu-1}\,, \\ \boldsymbol{a}_\nu = \mathcal{F}\,(\boldsymbol{b}_\nu)\ . \end{cases} \tag{10}$$

The iterative process starts with zero initial conditions, $\boldsymbol{a}_0 = \boldsymbol{0}$ and stops when the approximation error estimate

$$\boldsymbol{\delta}_\nu = \boldsymbol{a}_\nu - \boldsymbol{a}_{\nu-1} \tag{11}$$

is below a prescribed threshold. The longitudinal partitioning and relaxation has the main advantage of not requiring any coupled solution, since the two equations in (10) are just applied one at the time, until the solution estimate stabilizes through iterations.

B. Transverse Partitioning

We now introduce a transverse partitioning strategy, which is alternative or complementary to the longitudinal partitioning of Section III-A. This second partitioning scheme is motivated by the physical structure of most point to point links in state of the art technologies. In order to guarantee sufficient bandwidth for high-speed applications, several independent links are usually routed in close proximity for chip to chip communication. This leads to multiport interconnect systems, whose scattering matrix has a particular structure. Since there is no direct electrical connection between different links, which are only coupled through electromagnetic interactions occurring during the signal propagation along the channel, transmission and reflection coefficients are usually mugh larger in magnitude than near and far end crosstalks. Consequently, the scattering operator for such systems can be decomposed as

$$\mathcal{H} = \mathcal{D} + \mathcal{C} \tag{12}$$

where $\mathcal{D}$ collects all direct transmission and reflection coefficients, and operator $\mathcal{C}$ collects all crosstalks. Clearly, operator $\mathcal{D}$ is block-diagonal with 2×2 blocks after a suitable permutation depending on the port numbering is applied. In a good design, operator $\mathcal{C}$ is "small" in some sense with respect to $\mathcal{D}$ and can be interpreted as a second-order correction. We can restate (7) and (8) as

$$\begin{cases} \boldsymbol{\theta} &= \mathcal{C}\, \boldsymbol{a} \\ \boldsymbol{b} &= \mathcal{D}\, \boldsymbol{a} + \boldsymbol{\theta} \\ \boldsymbol{a} &= \mathcal{F}\,(\boldsymbol{b})\ , \end{cases} \tag{13}$$

where array $\boldsymbol{\theta}$ collects the crosstalk contributions, which can be interpreted as dependent correction sources applied to a set of decoupled channels. Figure 1c provides a graphical illustration of this transverse partitioning scheme.

We now introduce a transverse Waveform Relaxation scheme, which corrects solution estimates through iterations μ by applying the coupling terms $\boldsymbol{\theta}$ not instantaneously, but delayed by one iteration. We have system

$$\begin{cases} \boldsymbol{b}_\mu &= \mathcal{D}\, \boldsymbol{a}_\mu + \boldsymbol{\theta}_{\mu-1} \\ \boldsymbol{a}_\mu &= \mathcal{F}\,(\boldsymbol{b}_\mu) \\ \boldsymbol{\theta}_\mu &= \mathcal{C}\, \boldsymbol{a}_\mu\,. \end{cases} \tag{14}$$

which is solved with a suitable initial condition, e.g., $\boldsymbol{\theta}_0 = \boldsymbol{0}$. The main difficulty is the solution of the first two coupled equations in (14). On one hand, this problem is simpler than (10), since only two port variables are involved at the time (operator $\mathcal{D}$ is block diagonal). However, its solution still requires the exact solution of a nonlinear system. This is why we introduce a two-level partitionin scheme and relaxation in Section III-C.

C. Two-level partitioning

In this section, we combine the advantages of longitudinal and transverse partitioning into a single two-level Waveform Relaxation scheme. We start with (14) and we apply a further longitudinal partitioning and relaxation to the first two equations, as in Section III-A. We obtain

$$\begin{cases} \boldsymbol{b}_{\mu,\nu} = \mathcal{D}\, \boldsymbol{a}_{\mu,\nu-1} + \boldsymbol{\theta}_{\mu-1}\,, \\ \boldsymbol{a}_{\mu,\nu} = \mathcal{F}\,(\boldsymbol{b}_{\mu,\nu})\ , \end{cases} \tag{15}$$

where iteration indexes μ and ν correspond to transverse and longitudinal relaxation, respectively. Transverse relaxation forms an outer loop. At any step of this outer loop, i.e., for fixed μ, the outer relaxation sources $\boldsymbol{\theta}_{\mu-1}$ are known and fixed from previous outer iteration. Therefore, we can apply an inner longitudinal relaxation in order to solve individual channels. This inner loop is initialzed by using the solution estimate that is available at the end of previous outer iteration

$$\boldsymbol{a}_{\mu,0} = \boldsymbol{a}_{\mu-1,\mathcal{I}_{\mu-1}}\,, \tag{16}$$

where $\mathcal{I}_\mu$ is the total number of inner iterations for any fixed μ. Once the inner loop has terminated, the outer relaxation sources are updated according to

$$\boldsymbol{\theta}_\mu = \mathcal{C}\, \boldsymbol{a}_{\mu,\mathcal{I}_\mu} \tag{17}$$

and the process is repeated until convergence is achieved. A graphical illustration of the two-level partitioning scheme is available in Fig. 1d.

Convergence of inner and outer loops is detected by monitoring the respective residual norms with respect to a prescribed threshold ϵ

$$\xi_{\mu,\nu} = ||\boldsymbol{a}_{\mu,\nu} - \boldsymbol{a}_{\mu,\nu-1}|| \quad (18)$$

$$\delta_{\mu} = ||\boldsymbol{a}_{\mu,\mathcal{I}_\mu} - \boldsymbol{a}_{\mu-1,\mathcal{I}_{\mu-1}}|| \,. \quad (19)$$

The norm $\xi_{\mu,\nu}$ measures the amount of correction that is applied to the solution by the ν-th inner iteration, whereas the norm δ_μ measures the difference between two outer iterations, computed at the end of the inner loop. Throughout this work, we use the ∞-norm, i.e., the maximum deviation among all time samples of all port responses, in order to monitor uniform convergence.

D. Linear convergence analysis

We now address the convergence of the three proposed Waveform Relaxation schemes. The analysis is carried out in the frequency domain by assuming linear terminations, characterized by a scattering matrix $\boldsymbol{\Gamma}$ and internal source vector $\boldsymbol{\Upsilon}$. Only the main results are presented here, for a complete derivation and proof see [32]. The frequency-domain formulation of the two-level Waveform Relaxation scheme reads

$$\begin{cases} \boldsymbol{B}_{\mu,\nu} &= \mathbf{D}\,\boldsymbol{A}_{\mu,\nu-1} + \boldsymbol{\Theta}_{\mu-1}\,, \\ \boldsymbol{A}_{\mu,\nu} &= \boldsymbol{\Gamma}\boldsymbol{B}_{\mu,\nu} + \boldsymbol{\Upsilon}\,, \\ \boldsymbol{\Theta}_{\mu} &= \mathbf{C}\boldsymbol{A}_{\mu,\mathcal{I}_\mu}\,. \end{cases} \quad (20)$$

For simplicity, we assume that a constant number of inner iterations $\mathcal{I}$ is performed, independent on the outer iteration index μ. Defining

$$\mathbf{P}_{\mathcal{I}} = \mathbf{P} + (\boldsymbol{\Gamma}\mathbf{D})^{\mathcal{I}}\,(\mathbf{I} - \mathbf{P}) \quad (21)$$

where

$$\mathbf{P} = (\mathbf{I} - \boldsymbol{\Gamma}\mathbf{D})^{-1}\,(\boldsymbol{\Gamma}\mathbf{C})\,, \quad (22)$$

it is possible to prove by direct substitution [32] that the error between the solution estimate $\boldsymbol{A}_{\mu,\mathcal{I}}$ at the outer iteration μ and the exact solution $\boldsymbol{A}_{\text{exact}}$ reads

$$\boldsymbol{\mathcal{E}}_{\mu,\mathcal{I}} = \boldsymbol{A}_{\mu,\mathcal{I}} - \boldsymbol{A}_{\text{exact}} = -\mathbf{P}_{\mathcal{I}}^{\mu}\boldsymbol{A}_{\text{exact}}\,. \quad (23)$$

Convergence and consistency is thus guaranteed if the spectral radius (the magnitude of the largest eigenvalue) of operator $\mathbf{P}_{\mathcal{I}}$ is such that

$$\rho_{\max}\{\mathbf{P}_{\mathcal{I}}\} < 1\,. \quad (24)$$

This condition may be checked with a suitable frequency sampling process. Finally, we remark that the condition for convergence of pure transverse relaxation of Section III-B is recovered by solving exactly the inner loop, or equivalently by taking the limit for $\mathcal{I} \to \infty$, obtaining

$$\rho_{\max}\{\mathbf{P}\} < 1\,, \quad (25)$$

whereas convergence of the pure longitudinal relaxation of Section III-A is guaranteed when

$$\rho_{\max}\{\boldsymbol{\Gamma}\mathbf{H}\} < 1\,. \quad (26)$$

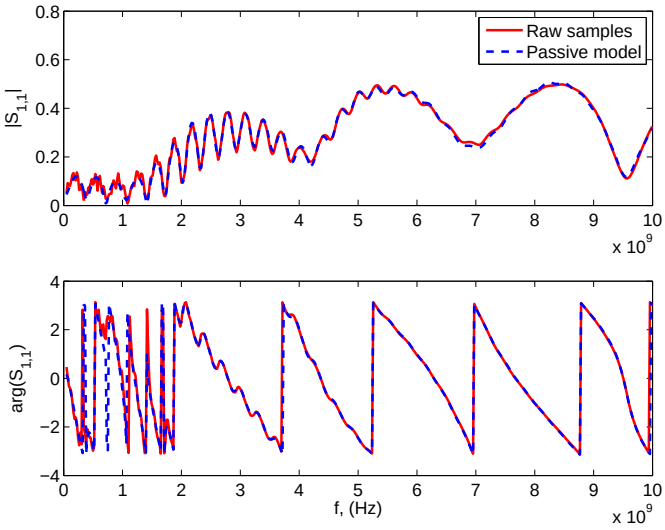

Fig. 3. Comparison between macromodel and raw scattering samples for S_{11} of Case III.

IV. Numerical results

The performance of the proposed Waveform Relaxation scheme is illustrated on four benchmarks. Case I is a simple structure with two segments of 9-conductor coupled lossy transmission lines separated by a discontinuity due to a via field. The other structures (Cases II–IV) are chip-to-chip links in real industrial products (courtesy of IBM), characterized by various topologies and electrical length. In particular: Case II connects a CPU to an I/O card through a PCB and a connector, Case III connects two CPUs on different PCB's through a flexible backplane, and Case IV connects two CPU's on the same PCB. In all cases the number of ports is $P = 18$, corresponding to a victim channel (ports 9 and 10) surrounded by eight aggressor channels. Figure 3 illustrates the accuracy of the computed passive Delay-Rational Macromodel for Case III by comparing one of its scattering responses to the raw frequency samples. The plot shows an excellent accuracy throughout the modeling bandwidth. Similar results were obtained for all cases.

Figure 4 depicts the spectral radius of iteration operator $\mathbf{P}_{\mathcal{I}}$ for different values of the inner iterations $\mathcal{I} = 2, 4, \infty$. A set of realistic linear terminations (40 Ω drivers and 1 pF receivers) were used for this analysis. In all cases the spectral radius does not exceed one, implying that convergence is expected, according to (24). Running the WR loops on a sequence of 500 bits led to the results depicted in Fig. 5, where the evolution of the inner loop error estimate (continuous line) and outer loop error estimate (dots) is plotted. A global iteration count is used in order to simplify visualization and interpretation. The figure panels show that the inner iterations converge quickly, although only $\mathcal{I} = 4$ inner iterations are used in this examples. Similarly, the error between successive outer iterations (dots) converges down to the the prescribed stopping threshold, in this case $\epsilon = 10^{-6}$.

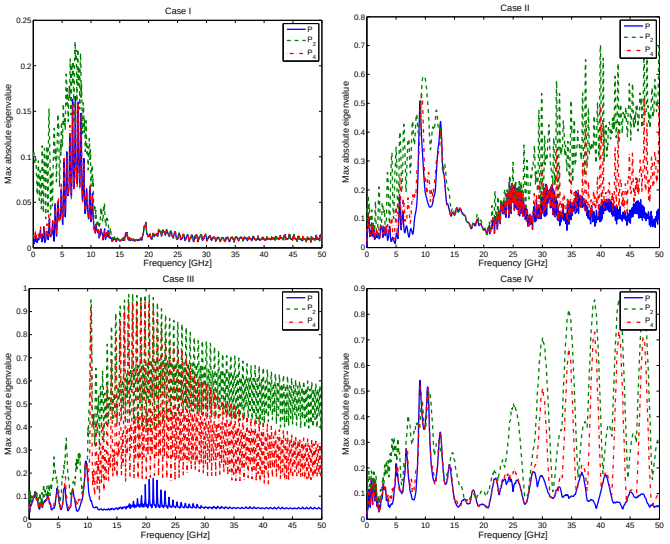

Fig. 4. Spectral radius of operator $\mathbf{P}_{\mathcal{I}}$ for $\mathcal{I} = 2, 4, \infty$ plotted versus frequency for all cases.

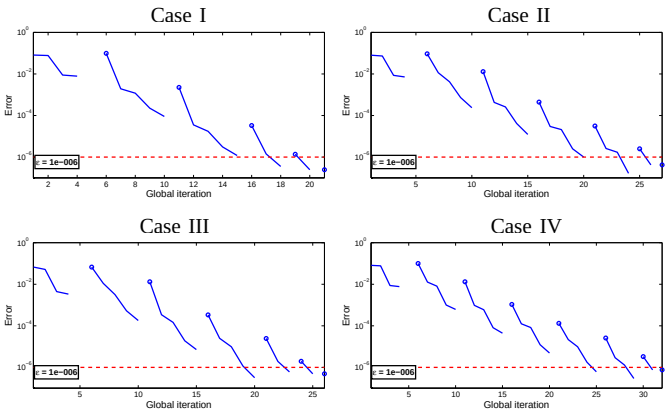

Fig. 5. Evolution of the inner (continuous line) and outer (dots) loop errors through iterations for all cases.

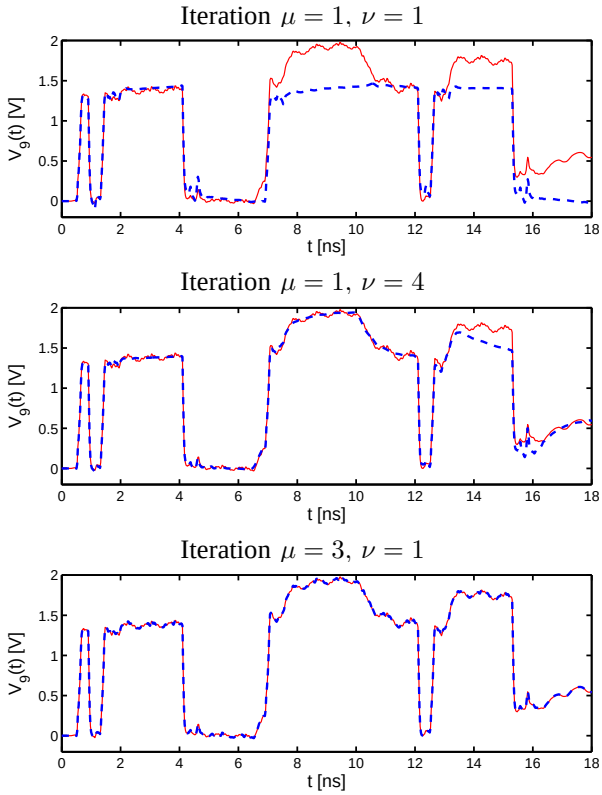

Fig. 6. Case II with nonlinear terminations. Solution at various WR iterations (blue dashed line) compared to the reference SPICE solution (red line).

TABLE I
COMPARISON OF SIMULATION TIMES REQUIRED BY SPICE AND BY DIFFERENT IMPLEMENTATIONS OF PROPOSED WR SCHEME TO RUN 1000 BITS ON CASE II.

Solver	CPU time	Speedup
SPICE	22m 55s	–
WR (Matlab)	62s	22 X
WR (C, 1 thread)	31s	44 X
WR (C, 9 threads)	5s	275 X

Figure 6 reports the evolution of the input voltage of the victim channel (Case II) through the first WR iterations. In this analysis, nonlinear and dynamic behavioral models of the MπLog class [31] were used for the drivers. It can be shown that such macromodels can be easily cast in the compact form (8), thus plugging naturally in our WR framework. These plots demonstrate that the final solution is indeed achieved by applying small iterative perturbations, thus providing a proof of concept of the proposed technique.

We conclude with some remarks on efficiency. Table I reports a comparison of the simulation times required by SPICE and by various implementations of our WR scheme to run a pseudo-random sequence of 1000 bits on Case II. In particular, we compare a prototypal Matlab implementation, a more advanced implementation coded in C language, and a preliminary parallelized version (OpenMP paradigm [33]) specifically tailored for multicore hardware, which was run using 9 concurrent threads. A major speedup is observed, particularly for the C-based parallel implementation. These preliminary results show excellent scalability of proposed WR scheme, which is capable of processing thousands of bits on fully coupled multiport channels ($P = 18$ ports) in seconds.

V. CONCLUSIONS

We presented three Waveform Relaxation (WR) schemes for transient simulation of complex multiport channels with possibly nonlinear terminations. These schemes are based on a longitudinal and/or transverse partitioning of the structure through suitable decoupling sources, which are relaxed through an iterative process. All schemes are consistent and converge quickly on a set of industrial benchmarks. Suitable conditions for convergence were also presented through a linear analysis.

Numerical results show that the same level of accuracy of

SPICE may be achieved in much faster runtime, especially if the WR scheme is parallelized for multicore hardware. The major speedup with respect to SPICE is mainly due to the optimized treatment of the small coupling terms due to inter-channel crosstalk, which are handled as second-order corrections. A generic SPICE solver is not aware of this structure, hence it is not able to exploit it to enhance numerical efficiency.

VI. Acknowledgement

The Authors are grateful to Dr. Kaller (IBM) for providing the channel characterization used in the paper. This work was supported in part by the Italian Ministry of University (MIUR) under a Program for the Development of Research of National Interest (PRIN grant #2008W5P2K).

References

[1] Beyene, W.T.; "Applications of Multilinear and Waveform Relaxation Methods for Efficient Simulation of Interconnect-Dominated Nonlinear Networks," *Advanced Packaging, IEEE Transactions on*, vol. 31, no. 3, pp. 637–648, Aug. 2008.

[2] Beyene, W.T.; Madden, C.; Jung-Hoon Chun; Haechang Lee; Frans, Y.; Leibowitz, B.; Ken Chang; Namhoon Kim; Ting Wu; Yip, G.; Perego, R.; "Advanced Modeling and Accurate Characterization of a 16 Gb/s Memory Interface," *Advanced Packaging, IEEE Transactions on*, vol. 32, no. 2, pp. 306–327, May 2009.

[3] Balamurugan, G.; Casper, B.; Jaussi, J.E.; Mansuri, M.; O'Mahony, F.; Kennedy, J.; "Modeling and Analysis of High-Speed I/O Links," *Advanced Packaging, IEEE Transactions on*, vol. 32, no. 2, pp. 237–247, May 2009.

[4] Sanders, A.; "Statistical Simulation of Physical Transmission Media," *Advanced Packaging, IEEE Transactions on*, vol. 32, no. 2, pp. 260–267, May 2009.

[5] S. Lin and E. S. Kuh, "Transient simulation of lossy interconnects based on the recursive convolution formulation," *IEEE Trans. Circuits Systems I*, vol. 39, pp. 879-892, Nov. 1992.

[6] A. Charest, D. Saraswat, M. Nakhla, R. Achar, N. Soveiko, "Compact Macromodeling of High-Speed Circuits via Delayed Rational Functions," *IEEE Microwave and Wireless Components Letters* Vol. 17, No. 12, pp. 828–830, Dec. 2007.

[7] A. Chinea, P. Triverio, S. Grivet-Talocia, "Delay-Based Macromodeling of Long Interconnects from Frequency-Domain Terminal Responses," *IEEE Transactions on Advanced Packaging*, Vol. 33, No. 1, pp. 246–256, Feb. 2010.

[8] A. Charest, M. Nakhla, R. Achar, D. Saraswat, N. Soveiko, I. Erdin, "Time Domain Delay Extraction-Based Macromodeling Algorithm for Long-Delay Networks," *IEEE Transactions on Advanced Packaging*, Vol. 33, No. 1, pp. 219–235, Feb. 2010.

[9] A. Charest, M. Nakhla, R. Achar, "Scattering Domain Passivity Verification and Enforcement of Delayed Rational Functions," *IEEE Microwave and Wireless Components Letters*, Vol. 19, No. 10, Oct. 2009, pp. 605–607.

[10] A. Chinea, S. Grivet-Talocia, P. Triverio, "On the performance of weighting schemes for passivity enforcement of delayed rational macromodels of long interconnects," in *IEEE 18th Conf. on Electrical Performance of Electronic Packaging and Systems*, Portland (Tigard), Oregon, Oct. 19–21, 2009.

[11] A. Charest, M. Nakhla, R Achar, C. Chen, "Passivity verification and enforcement of delayed rational function macromodels from networks characterized by tabulated data," in *IEEE Workshop on Signal Propagation on Interconnects, 2009. SPI'09*, pp. 1–4, May 12–15, 2009.

[12] A. Chinea, S. Grivet-Talocia, D. Deschrijver, T. Dhaene, L. Knockaert, "On the construction of guaranteed passive macromodels for high-speed channels," *Design, Automation and Test in Europe (DATE 10)*, Dresden (Germany), pp. 1142-1147, March 8-12, 2010.

[13] A. Chinea, S. Grivet-Talocia, H. Hu, P. Triverio, D. Kaller, C. Siviero, M. Kindscher, "Signal Integrity Verification of Multi-Chip Links using Passive Channel Macromodels," accepted for publication in *IEEE Transactions on Advanced Packaging*, 2010.

[14] A. Chinea, P. Triverio, and S. Grivet-Talocia, "Passive delay-based macromodels for signal integrity verification of multi-chip links," in *14th IEEE Workshop on Signal Propagation on Interconnects, Hildesheim, Germany*, May 9–12, 2010.

[15] V. Loggia and S. Grivet-Talocia, "A two-level waveform relaxation approach for fast transient simulation of long high-speed interconnects," in *IEEE* 19^{th} *Topical Meeting on Electrical Performance of Electronic Packaging and Systems (EPEPS 2010), Austin, TX*, October 24–27, 2010.

[16] F. Y. Chang, "The generalized method of characteristics for waveform relaxation analysis of lossy coupled transmission lines," *IEEE Trans. Microwave Theory Tech.*, vol. 37, pp. 2028-2038, Dec. 1989.

[17] F.C.M. Lau, "Improvements in the Waveform Relaxation Method Applied to Transmission Lines", *IEEE Transactions on Computer-Aided Design of Integrated Circuits and Systems*, Vol.13, No.11, Nov.1994, pp.1409–1412.

[18] E.Lelarasmee, A.E.Ruehli, A.L.Sangiovanni-Vincentelli, "The Waveform Relaxation Method for Time-Domain Analysis of Large Scale Integrated Circuits", *IEEE Transactions on Computer-Aided Design of Integrated Circuits and Systems*, Vol. 1, N. 3, July 1982, pp. 131–145.

[19] P.Debefve, J.Beetem, W.Donath, H.Y.Hsieh, F.Odeh, A.E.Ruehli, P.Wolff, Sr., and J. White, "A large-scale MOSFET circuit analyzer based on waveform relaxation," *IEEE Int. Conf. Computer Design*, Rye, NY, Oct. 1984.

[20] J.K.White and A.L.Sangiovanni-Vincentelli, *Relaxation Technique for the Simulation of VLSI Circuits*. Norwell, MA: Kluwer Academic, 1987.

[21] Nakhla, N.M.; Ruehli, A.E.; Nakhla, M.S.; Achar, R.; "Simulation of coupled interconnects using waveform relaxation and transverse partitioning," *IEEE Transactions on Advanced Packaging*, vol. 29, no. 1, pp. 78–87, Feb. 2006

[22] Paul, D.; Nakhla, N.M.; Achar, R.; Nakhla, M.S.; "Parallel Simulation of Massively Coupled Interconnect Networks," *IEEE Transactions on Advanced Packaging*, vol. 33, no. 1, pp. 115–127, Feb. 2010.

[23] Martin Gander; Mohammad Al-Khaleel; Albert E. Ruehli; "Waveform Relaxation Technique for Longitudinal Partitioning of Transmission Lines,"in *IEEE* 15^{th} *Topical Meeting on Electrical Performance of Electronic Packaging, Scottsdale, Arizona*, pp. 207–210, Oct. 23–25, 2006.

[24] R.Wang, O.Wing, "Transient Analysis of Dispersive VLSI Interconnects Terminated in Nonlinear Loads", *IEEE Transactions on Computer-Aided Design*, Vol.11, N.10, Oct.1992, pp. 1258–1277.

[25] A.Lumsdaine, M.W.Reichelt, J.M.Squyres, J.K.White, "Accelerated Waveform Methods for Parallel Transient Simulation of Semiconductor Devices", *IEEE Transactions on Computer-Aided Design of Integrated Circuits and Systems*, Vol. 15, N. 7, July 1996, pp. 716–726.

[26] G.D.Gristede, A.E.Ruehli, C.A.Zukowski, "Convergence Properties of Waveform Relaxation Circuit Simulation Methods", *IEEE Transactions on Circuits and Systems-I: Fundamental Theory and Applications*, Vol.45, No.7, July 1998, pp. 726–738.

[27] Yao-Lin Jiang, "A General Approach to Waveform Relaxation Solutions of Nonlinear Differential-Algebraic Equations: The Continuous-Time and Discrete-Time Cases", *IEEE Transactions on Circuits and Systems-I: Regular Papers*, Vol.51, No.9, Sept.2004, pp. 1770–1780.

[28] I.M.Elfadel, "Convergence of Transverse Waveform Relaxation for the Electrical Analysis of Very Wide Transmission Line Buses", *IEEE Transactions on Computer-Aided Design of Integrated Circuits and Systems*, Vol.28, No.8, 2009, pp.1150–1161.

[29] N.Nakhla, A.E.Ruehli, M.S.Nakhla, R.Achar, C.Chen, "Waveform Relaxation Techniques for Simulation of Coupled Interconnects With Frequency-Dependent Parameters", *IEEE Transactions on Advanced Packaging*, Vol.30, N.2, 2007, pp. 257–269.

[30] M.J.Gander, A.E.Ruehli, "Optimized waveform relaxation solution of electromagnetic and circuit problems", in *IEEE 19th Conference on Electrical Performance of Electronic Packaging and Systems (EPEPS)*, 25–27 Oct. 2010, Austin, TX, USA, pp. 65–68.

[31] I.S.Stievano, I.A.Maio, F.G.Canavero, "M[pi]log, Macromodeling via Parametric Identification of Logic Gates," *IEEE Transactions on Advanced Packaging*, Vol. 27, No. 1, pp. 15–23, Feb. 2004.

[32] V.Loggia, S.Grivet-Talocia, "Transient simulation of complex high-speed channels via Waveform Relaxation", submitted to IEEE Trans. Advanced Packaging, 2010.

[33] OpenMP Architecture Review Board, *OpenMP C and C++ Application Program Interface - Version 2.0*, Mar. 2002. Available: http://www.openmp.org/mp-documents/cspec20.pdf.